

**Title:** Design of a Braiding Machine to Produce Wide, Flat Woven Structures  
at a Significantly Increased Production Rate

**Principal Investigators:** R.P. Walker, D.M. Beale, S. Adanur, R.M. Nelms and R.M. Broughton, Jr.

**Goal Statement:**

The primary goal of this project is to develop a multi-phase weaving process that offers potential for significantly increasing the production rate of woven fabric. To accomplish this goal, the mechanics of braiding must be defined and the limitation imposed by yarn-to-yarn friction during braiding must be overcome to allow forming of compact structures.

**Abstract:**

An interdisciplinary research team of five faculty (3 TE, 1 ME & 1 EE), over the life of the project, have involved six graduate students and ten undergraduate students in projects to investigate a technology that offers a break through to increased weaving production rate using a braiding, 'yarn slip interlacing' concept to produce a tubular structure which when bias slitted would make a flat woven fabric. Design drawings for two machine test models have been completed and work is continuing on a novel slip shrouded weft yarn package and an electromagnetically activated warp yarn deflection mechanism. A defining manuscript on the mechanics of braiding is nearing completion and solutions to overcome limits imposed by yarn-to-yarn friction on the compactness of a braided structure are being developed for study.

**Body of Report:**

**Research Team Activity**

The research team consists of faculty from Textile Engineering (3 members), Mechanical Engineering (1 member), and Electrical Engineering (1 member) currently working with four graduate students (1 PhD ME, 1 MS ME, 1 MS EE, and 1 MS TE) and several undergraduate students doing senior design projects. The following student projects have been developed:

<u>Zhang, Qiang (PhD, ME)</u>	"A Study of the Mechanics Model of Yarn Interlacing by Braiding", an incomplete study.
<u>Hunt, Richard (MS, EE)</u>	"Analysis, Design and Optimization of an Electromagnetic Yarn Deflection Actuator Mechanism for a Novel Yarn Slip Interlacing System", an incomplete study.
<u>Sartain, Stephen (MS, TS)</u>	"A Comparison of the Structural Characteristics and Behavioral Properties of Interlaced Fabrics Produced by Braiding and Weaving", an unpublished thesis, 101 pages.
<u>Vickers, Daniel (MS, ME)</u>	"Analysis, Design and Optimization of a New Process for Interlacing Yarn", an incomplete study.
<u>Burst, Brian (BS, ME)</u>	"Design of Deflector to Raise Threads Over Stationary Barriers on a Weaving Machine", an unpublished senior advanced project report, 29 pages.
<u>McLean, Matthew (BS, ME)</u>	"Ring System for the Braider-Loom", an unpublished senior advanced project report, 11 pages.
Bedell, Ware (BS, ME); Kruse, Grant (BS, ME) and <u>Redman, Kevin (BS, ME)</u>	"Development of a Braiding Loom Prototype", an unpublished senior advanced project report, 26 pages and six appendices.

<u>Johnson, Joseph (BS, TMT)</u>	"Development of Procedures and Testing Apparatus to Study Yarn Interaction in a Braided Structure", an unpublished senior research report, 31 pages.
<u>Cofield, Melanie (BS, TE)</u>	"A Study of Interacting Forces Between Two Sets of Interlacing Yarns", an incomplete senior design project.
<u>Reynolds, Jeffrey (BS, TMT)</u>	"A Study of the Force Required to Ravel Yarns from a Woven Structure", an incomplete senior research project.

### Model Test Machine

A model test machine has been designed to demonstrate a novel 'Yarn Slip Interlacing' concept which is proposed as the braiding component of any future weaving machine based on this work. An assembly drawing has been completed as shown in Figure 1. It can be seen in Figure 1 that the test machine is designed to be driven by three coaxial, hollow shafts. The inner shaft drives the fabric take-up and rotating mandrel synchronously. The middle shaft would rotate the inner weft yarn spools if movement of this system of yarns was desirable. Currently, keeping the weft yarn packages stationary is the operation of choice, since control of yarn deflection by electromagnets is being considered. The outer shaft drives the outer warp yarn spools which are set on an inner ring of a large bearing. The inner ring is connected to the outer shaft by several support arms. The warp spools are held by the outer ring of the bearing. The take-up mechanism is designed to rotate with the mandrel on a separate large bearing. The test machine was designed to permit separate control of the speeds for rotation of the weft spools, rotation of the warp spools, linear fabric take-up and mandrel rotation. Different combinations of these speed parameters will result in different production rates and different braid geometry. The various possibilities or machine configurations are illustrated in Table I. Element drawings with required tolerances have not been completed. Most of the machine parts were chosen from standard catalogs with the exception of the key components, a 'slip shrouded' weft yarn package and an electromagnetically activated yarn deflection mechanism, which are being developed separately. A patent disclosure on the 'Yarn Slip Interlacing' concept (see Figure 2) has been submitted to Auburn University Administration. It has been suggested that funding for the building of this test model should be sought outside the NTC.

An extensive undergraduate Senior Advanced Design Project has been completed by Bedell, Kruse and Redman. This project involved conversion of a 30-inch diameter, circular single knitting machine into a braiding machine incorporating a rotating mandrel, a rotating warp yarn system and stationary weft yarn insertion devices. Complete details for this conversion including all pertinent engineering drawings were produced as presented in the lengthy report alluded to above.

### The 'Yarn Slip Interlacing' (YSI) Concept

Work is continuing separately on the analysis, design and optimization of the slip device and the yarn deflection mechanism. These components will be consolidated during further research to test the frequency and reliability of controlled interlacing between two sets of yarns.

#### The 'Slip' device

A literature search concerning yarn-to-surface and yarn-to-yarn friction and wear of sliding yarns has been completed and is included in a thesis scheduled for completion next month. An apparatus to determine forces involved with sliding yarns across various contours and surfaces has been designed as illustrated in Figure 3. The experimental set-up consists of the means for applying tension to yarn, moving yarn in a horizontal plane, positioning yarn in the vertical direction and measuring yarn displacement in both directions. This apparatus has been used to collect fifteen data sets taken over various cycle frequencies using four surface profiles. Profiles were made of 3/16" plexiglass using a three-axis milling machine controlled by a computer program written especially for this work. The tool bit width, depth of the cut and two eccentric radii are coded by the program and down-loaded to the milling machine which makes four path cuts increasing in depth by 0.5" increments. In

these experiments, point contact between a yarn and the 'slip' device surface is assumed. The profile is made to represent the shape of a cross-section of the inner (weft) yarn package in the vertical plane along the direction perpendicular to the moving (warp) yarn. The initial experiment was filmed using high-speed photography so data could be calculated on the normal force exerted by the yarn on the surface of the elliptical profile. Digitizing three points per frame of the film allows calculation of the angle a yarn makes as it contacts a surface. Digitizing this data is accomplished with a VCR, a computer and software which saves images to a disk. These film data are combined with the data collected from a tensiometer and position sensor. A dynamic simulation of the experiments was programmed to generate theoretical data for correlation to empirical results. Programming of the dynamic simulation was accomplished using the MATLAB (version 4.1), a matrix manipulation software package on the Sun work station network. The program is being used to generate theoretical curves and to process empirical data. To use the theoretical simulation, it was necessary to determine the tension and friction characteristics of yarns. The denier and stress-strain curves were obtained on twenty yarn specimens using the Instron Tensile Tester. A fourth order curve fit (99.962% correlation) of the averaged grams per denier-% elongation curves was used to determine the polynomial function which most closely matched the yarn tension characteristics. This function was used in the theoretical program for calculation of the tension of the yarn for a given amount of elongation based on the yarn geometry. This tension was compared to the measured experimental tension.

Correlation of the theoretical values with the experimental values was accomplished using an intrinsic function of the MATLAB software called CORRCOEF (X,Y). This function determines the correlation coefficients of two equal length vectors. The theoretical values represented one vector and the empirical values represented the other vector. In general, correlation coefficients were observed to be near 0.9 (90%) for all theoretical and experimental data sets. The high degree of correlation means that the theoretical simulation can be used to predict results for situations similar to those in the experiment. Therefore, the basis for optimizing the shape of the slipped yarn package has been established. Graphical output using the MATLAB program is underway. The program plots the yarn tension, frictional force and position of the yarn/surface contact point as functions of time. Also, the parametric relationships of the friction study with respect to the eccentricities of the elliptical profiles will be plotted. A publication is being developed for submission to the Textile Research Journal as well as the final draft of a thesis covering this work.

### **The Yarn Deflector**

The primary accomplishment of the past year was writing and testing a program to predict the reaction time of an electromagnetically activated deflector for the yarn slip interlace device. Although the electromagnetic force equations for a solenoid can be solved in closed form, there is no closed form solution for the system mechanical dynamics. Therefore a program was written to solve the system dynamics. The program predicts reaction times based on various system parameters such as solenoid size, size and stiffness of the deflector, and the supply voltage. In all there are ten parameters that influence reaction time. Reaction time was chosen as the variable of interest since it will determine how fast fabric can be produced. Assuming a deflector can operate at 50 Hz, each deflector would accomplish 3000 interlacings per minute. The way this rate is developed; either by having a slowly rotating, dense warp sheet or a faster, less dense warp sheet; is a trade off; but the number of warp yarns times rpm cannot exceed the deflector operating rate in interlacings per minute.

---

For movement of components, mechanical methods offer the fastest operational rate; unfortunately, they are not as controllable or reliable as electrical devices. Despite the relative slowness of electrical devices, there are techniques to obtain deflector operating speeds greater than 200 Hz which would enable a machine to easily outproduce existing looms. However, most of these techniques utilize costly materials or complex mechanical linkages, so the goal in this portion of the research was to investigate the possibility of using low cost materials and yet still meet a desirable operating speed. In order to keep the mechanical design as simple as possible, it was decided to utilize some sort of force-at-a-distance approach, so electromagnets were chosen as the device to use. Theoretically, a sufficiently large electromagnet could easily generate the force required to move the deflector in a given time. Unfortunately, the larger the electromagnet the longer it takes for the magnetic field

of the coil to build up, so there is a trade off between magnetic force reaction time and field build-up time. Consequently, there is an optimum size that will produce the fastest total reaction time for a given deflector. The various outputs from the program can be compared and plotted to determine the optimum size.

A small test apparatus was built to determine the accuracy of predicted results in which prototype deflectors and deflection distance can be varied, and sample electromagnets, using cores obtained from Elna Ferrite tested for applicability. For each configuration, the first step in the test procedure is to measure single cycle deflection reaction time and coil current using a digital storage oscilloscope. The deflector was configured as a contact switch, and by comparing the deflector switch cycle with the coil current, the components of the reaction time can be compared. Then, a solid-state electronic switch is used to operate the deflector at varying frequencies to investigate operational characteristics. Testing of the electromagnets is continuing, but the initial results indicate a good correlation between predicted and actual reaction times.

Some interesting behavior has been observed so far. The magnetic field is proportional to the current, and the current should increase at a decreasing exponential rate, so the greater the power supply voltage the faster the field should build up. Experimentally that turns out to be true only up to a limit beyond which the field build-up rate stays constant. This implies that a power supply only needs to be large enough to create the maximum rate, and therefore large voltages are unnecessary. Another feature that requires further investigation is how the natural frequency of the deflector affects the frequency of operation. It appears that the deflector works best when operated at a rate that is either a whole number fraction or multiple of its natural frequency. Finally, some deviations in the deflector model have been noted. In the program, the deflector is modeled as a small mass attached to a spring (e.g. the force opposing deflector motion is represented as a spring). This relationship holds true for small deflector distances, but is not valid for large distances where the force becomes highly non-linear. Further work is needed to determine the practical limits for deflection distances and where the point of non-linearity is in relation to deflector size.

The final area where some work has been done is in designing an energy recovery circuit for the electromagnet. The electrical energy stored in the electromagnet is quite significant and simply dissipating it in resistive losses is costly. A circuit to reuse the energy is being investigated from a theoretical perspective. Once an adequate circuit is designed, simulations will be performed and a prototype built to verify feasibility.

Figure 4 is a schematic of a typical electromagnet which might be used with the deflector of the yarn slip interlacing device. All labeled elements are design variables to be optimized for a particular machine and deflector design. Using the program developed in this research, plots can be made showing how each parameter affects deflector reaction time and operating frequency. Figure 5 is a plot of how the relative permeability of the magnet core influences reaction time for various inner radius dimensions. As can be seen in Figure 5, in all cases an increase in relative permeability decreases reaction time, though at a decreasing rate. Since material cost increases with relative permeability, there is a point beyond which the small increase in reaction time due to increasing relative permeability is not cost effective. The point of optimization of relative permeability is different for each inner radius. A second plot is presented in Figure 6 showing how changing the inner radius affects reaction time for different betas. Once again there is an obvious optimum point around 2-3 mm. Although bigger betas, and therefore bigger electromagnets, produce more powerful magnetic fields, they also have a large inductance that slows down the total reaction time. The extra length, beyond the optimum point, does not produce enough additional magnetic field to offset the increased inductance. Other plots show that the optimum value for alpha is about 5, the value used in these Figures. From these early plots it appears that a short, wide electromagnet may be optimum.

#### Mechanics of Braiding

One refereed publication entitled "Weaving Technology - What Next?" has been published (Melliand Textilberichte; Vol. 75, No. 4; April, 1994; pages 267 and 272) and a second publication entitled "Structural Analysis of Two Dimensional Braided Fabric" has been submitted to the Journal of the Textile Institute.

Cover factor is considered as a function of braid angle, helical length, braid diameter, number of yarns and yarn diameter. In the braiding process each of these parameters can be fixed and the other parameters are governed by geometric equations. As shown in Figure 7, when the mandrel diameter is a constant, the cover factor increases as the braid angle increases. Furthermore, the influence of helical length on cover factor is presented in Figure 8, where it can be seen that the stable jammed condition of a braid occurs at the minimum helical length when the braid angle is 45 degrees. A dense fabric has a small helical length and high crimp which tends to decrease the cover factor. When using the model to calculate cover factor for a monofilament yarn, the maximum value of cover factor is 0.82. As indicated by Figure 8, the change in helical length allows a change from two unstable jammed braids (compression jammed state and extension jammed state) to one stable jammed state when the braid angle is maintained at 45 degrees. The cover factor decreases with mandrel diameter when the speed of the braiding machine is held constant, as shown in Figure 9.

Initial experimental data was obtained by making braids from several different yarns. The braids were made with different braid angles, helical lengths and braid diameters. Machine parameters were measured to compare with results obtained from kinematic relationship formulas. The experiment revealed that formation of the braid is highly influenced by the mechanics relationships. A high cover factor, or compact structure, is not possible with most of the yarn types used because of high yarn frictional forces. Since the braiding process relies entirely on tension to 'pull' yarns into a crimped state, the yarn-to-yarn friction caused by interlacing a large number of yarns restricts the progress of yarns creating less than desirable cover or compactness in the structure. A comparison of the experimental data and the theoretical data are presented in Figure 10. This is an early indication that the theoretical models are fairly accurate.

Solutions to the problem of braid compactness are being considered such as yarn lubrication to reduce yarn friction, the introduction of vibration to change yarn friction from the static to the dynamic state, off-line fabric compaction and others. Also a test device to simulate the action of braiding is being developed to study the force required to extract yarns from a compact woven structure (the opposite of the force required to form the fabric).

#### Braided and Woven Fabric Comparison

Several attempts were made to produce acceptable braided fabrics for direct comparison to similarly constructed woven fabrics. Interlacing friction between yarns during braiding restricted formation of acceptable fabrics with most yarn types (coarse cotton, fine cotton, nylon carpet, pvc coated and slub yarns) except polypropylene slit-film, wide ribbon yarns. Properties of the braided fabric produced with this slit film yarn are compared to a woven fabric of similar construction are presented in Table II. As shown in Table II, cover factor for the two fabrics was the same, the woven fabric had slightly more crimp and the braided fabric was somewhat heavier. Values for tensile strength, elongation, shear strength and tear strength were normalized for fabric weight. It may be concluded from this one comparison that this flat woven fabric produced by slitting a braided tubular structure has tensile properties about the same as those of a woven fabric produced by conventional weaving. Only the elongation of the two samples appears to be noticeably different and part of that difference may be explained by the difference in crimp of the two fabrics. A full thesis has been produced including recommendations for future work. It is recommended that future comparison of braided and woven fabrics be done on samples produced from exactly the same yarn and that braided samples be made on a machine designed specifically to produce flat woven fabric as replacement fabric for conventionally woven fabric. Flat woven fabrics produced on existing braiding machines are too narrow for direct comparison to loom woven goods using standard test methods. The problem related to compactness of braided structures must also be solved before reasonable samples can be produced by braiding.

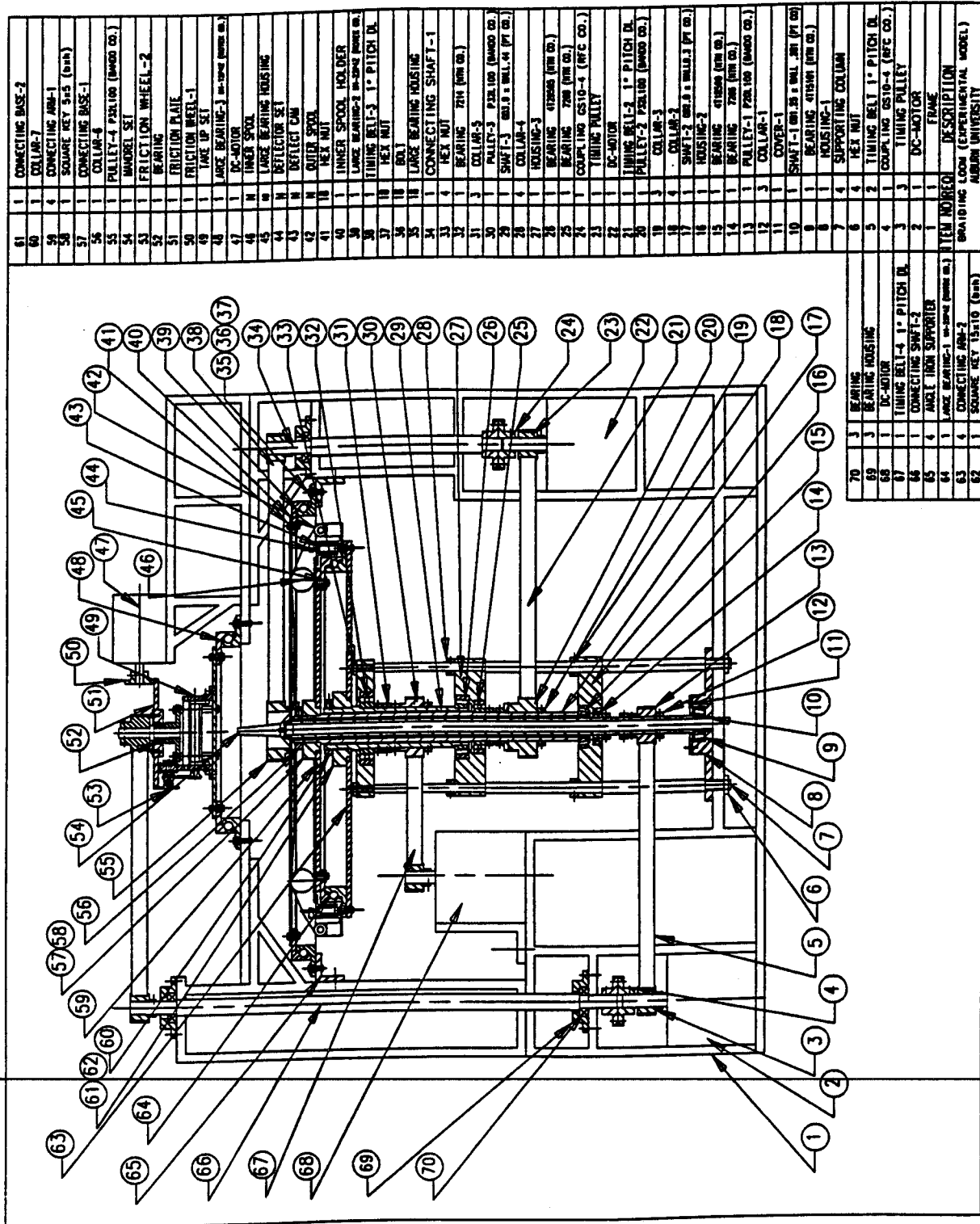


Figure 1. Experimental Model of Braiding Test Loom

61	CONNECTING BASE-2
60	COLLAR-7
59	CONNECTING ARM-1
58	SQUARE KEY 5x5 (brk)
57	CONNECTING BASE-1
56	COLLAR-6
55	PULLEY-4 PDL100 (WOOD CO.)
54	MANDREL SET
53	FRICTION WHEEL-2
52	BEARING
51	FRICTION PLATE
50	FRICTION WHEEL-1
49	TAKE UP SET
48	LARGE BEARING-3 IN-SIDE (WOOD CO.)
47	DC-MOTOR
46	INNER SPOOL
45	LARGE BEARING HOUSING
44	M REFLECTOR SET
43	M REFLECTOR CAN
42	M OUTER SPOOL
41	HEX NUT
40	INNER SPOOL HOLDER
39	LARGE BEARING-2 IN-SIDE (WOOD CO.)
38	TIMING BELT-3 1" PITCH DL
37	ROLI
36	HEX NUT
35	LARGE BEARING HOUSING
34	CONNECTING SHAFT-1
33	HEX NUT
32	BEARING ZIN (WOOD CO.)
31	COLLAR-5
30	PULLEY-3 PDL100 (WOOD CO.)
29	SHAFT-3 60x8x3 WLL.4 (PT CO.)
28	COLLAR-4
27	HOUSING-3
26	BEARING 412000 (WOOD CO.)
25	BEARING 700 (WOOD CO.)
24	COUPLING GSTD-4 (RFC CO.)
23	TIMING PULLEY
22	DC-MOTOR
21	TIMING BELT-2 1" PITCH DL
20	PULLEY-2 PDL100 (WOOD CO.)
19	COLLAR-3
18	COLLAR-2
17	SHAFT-2 60x8x3 WLL.3 (PT CO.)
16	HOUSING-2
15	BEARING 412000 (WOOD CO.)
14	BEARING 700 (WOOD CO.)
13	PULLEY-1 PDL100 (WOOD CO.)
12	COLLAR-1
11	COVER-1
10	SHAFT-1 60x8x3 WLL.3 (PT CO.)
9	BEARING 412000 (WOOD CO.)
8	HOUSING-1
7	SUPPORTING COLUMN
6	HEX NUT
5	TIMING BELT 1" PITCH DL
4	COUPLING GSTD-3 (RFC CO.)
3	TIMING PULLEY
2	DC-MOTOR
1	FRAME
ITEM NUMBER DESCRIPTION	
BRAIDING LOOM (EXPERIMENTAL MODEL)	
AUBURN UNIVERSITY	

70	3	BEARING
69	3	BEARING HOUSING
68	1	DC-MOTOR
67	1	TIMING BELT-4 1" PITCH DL
66	1	CONNECTING SHAFT-2
65	4	ANGLE IRON SUPPORTER
64	4	LARGE BEARING-1 IN-SIDE (WOOD CO.)
63	4	CONNECTING ARM-2
62	1	SQUARE KEY 15x10 (brk)

Table I. Crossing Angle and Interlacing Speed Calculation for Various Braiding Machine Configurations

cases	yarns on mandrel	unit cell	braid layout	crossing angle	interlacing speed IS (interlacings/sec)	comment
$\Omega = 0$ $\omega_1, \omega_2 < 0$ $\omega_1 \neq \omega_2$				$\alpha = 2 \tan^{-1} \frac{\omega_1 D}{2V}$	$IS = \frac{2(\omega_1 - \omega_2)}{2\pi}$ $= \frac{2\omega_1}{\pi}$	Mandrel is stationary. Two sets of spools run in opposite directions at the same speed. It is easy to get 90° braid angle. Unit cell is symmetrical. Production rate is high.
$\Omega = 0$ $\omega_1, \omega_2 < 0$ $\omega_1 \neq \omega_2$				$\alpha = \tan^{-1} \frac{\omega_1 D}{2V}$ $+ \tan^{-1} \frac{\omega_2 D}{2V}$	$IS = \frac{\omega_1 + \omega_2}{\pi}$	Mandrel is stationary. Two sets of spools run in opposite directions at different speed. The unit cell is not symmetrical. The fabric needs to be skewed. Production rate is high.
$\Omega = 0$ $\omega_1, \omega_2 > 0$ $\omega_1 \neq \omega_2$				$\alpha = \tan^{-1} \frac{\omega_1 D}{2V}$ $- \tan^{-1} \frac{\omega_2 D}{2V}$	$IS = \frac{\omega_1 - \omega_2}{\pi}$	Mandrel is stationary. Two sets of spools run in the same direction. Crossing angle is small. Fabric needs to be skewed. Interlacing speed is low. If $\omega_1 = \omega_2$ IS=0, there is no interlacing.
$\Omega > 0$ $\omega_1, \omega_2 > 0$ $\omega_1 \neq \omega_2$				$\alpha = \tan^{-1} \frac{(\omega_1 - \Omega) D}{2V}$ $- \tan^{-1} \frac{(\omega_2 - \Omega) D}{2V}$	$IS = \frac{\omega_1 - \omega_2}{\pi}$	Mandrel rotates. Two sets of spools run in the same direction. Braid angle is influenced by $\Omega$ . Interlacing speed is the same as case 3.
$\Omega > 0$ $\omega_1, \omega_2 < 0$				$\alpha = \tan^{-1} \frac{(\omega_1 - \Omega) D}{2V}$ $+ \tan^{-1} \frac{(\omega_2 + \Omega) D}{2V}$	$IS = \frac{\omega_1 + \omega_2}{\pi}$	Mandrel rotates. Two sets of spools run in opposite directions. Interlacing speed is the same as case 2. If $\Omega$ is larger than $\omega_1$ , the crossing angle is similar to case 3.
$\Omega > 0$ $\omega_2 = 0$				$\alpha = \tan^{-1} \frac{(\omega_1 - \Omega) D}{2V}$ $+ \tan^{-1} \frac{\Omega D}{2V}$	$IS = \frac{\omega_1}{\pi}$	Mandrel rotates in the same direction as $\omega_1$ . $\omega_2 = 0$ . I.e. one set of spools is stationary. This case makes it possible to use electrically controlled deflectors. The interlacing speed depends only on $\omega_1$ since relative speed is $\omega_1$ .
$\Omega > 0$ $\omega_1 < 0$ $\omega_2 = 0$				$\alpha = \tan^{-1} \frac{(\omega_1 + \Omega) D}{2V}$ $- \tan^{-1} \frac{\Omega D}{2V}$	$IS = \frac{\omega_1}{\pi}$	Mandrel rotates in the opposite direction as $\omega_1$ . $\omega_2 = 0$ . This case has smaller braid angle than case 6. The interlacing speed is the same as case 6.

\*\* V is take-up speed.  $\omega_1$  and  $\omega_2$  are the absolute rotational speed of the two sets of spools. Production rate here is represented by interlacing speed. The mandrel speed  $\Omega$  has no contribution to the relative speed between  $\omega_1$  and  $\omega_2$ . Therefore, it does not influence interlacing speed. However  $\Omega$  does determine the braid angle and the production rate in terms of yards / minute.

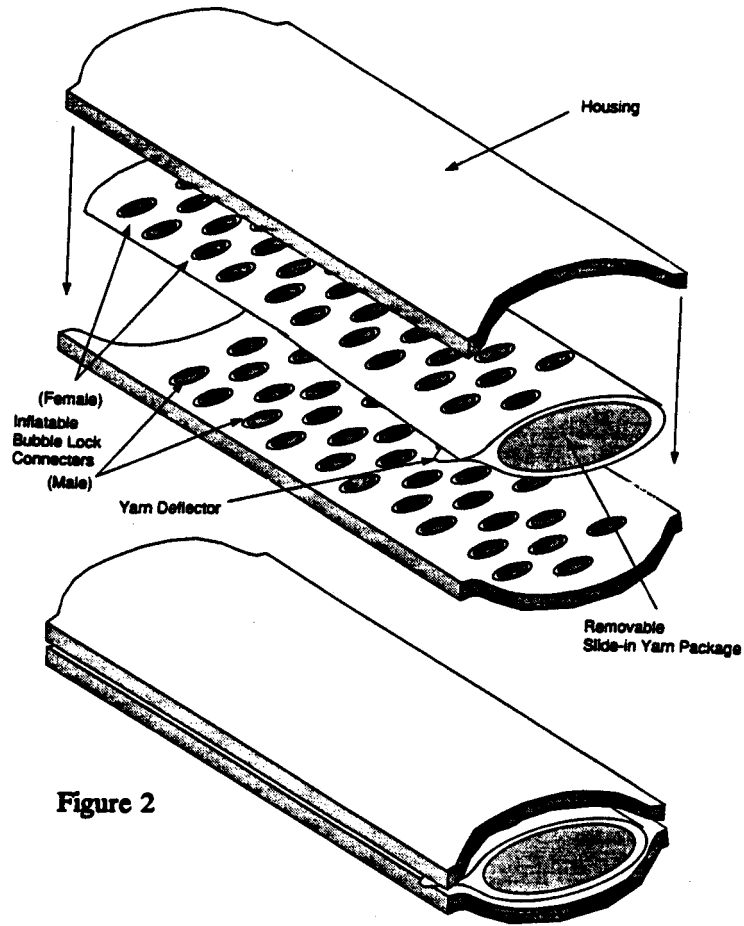


Figure 2

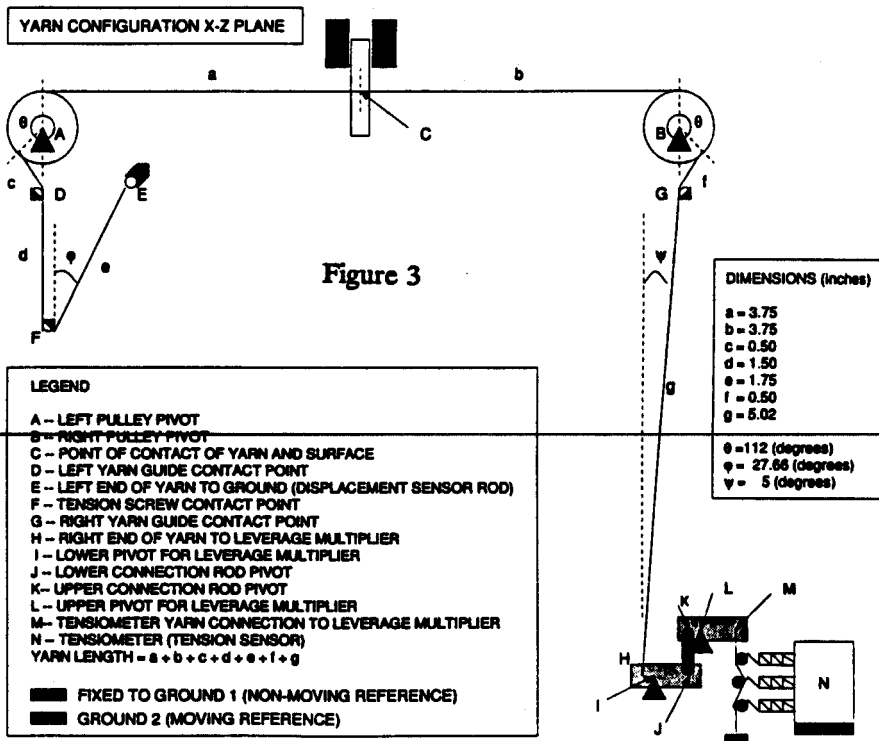
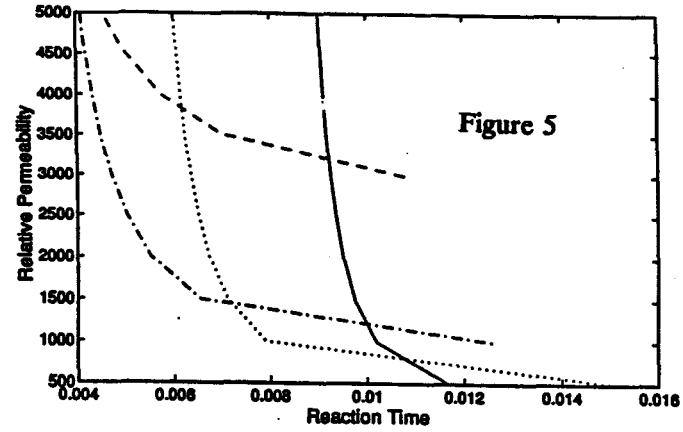
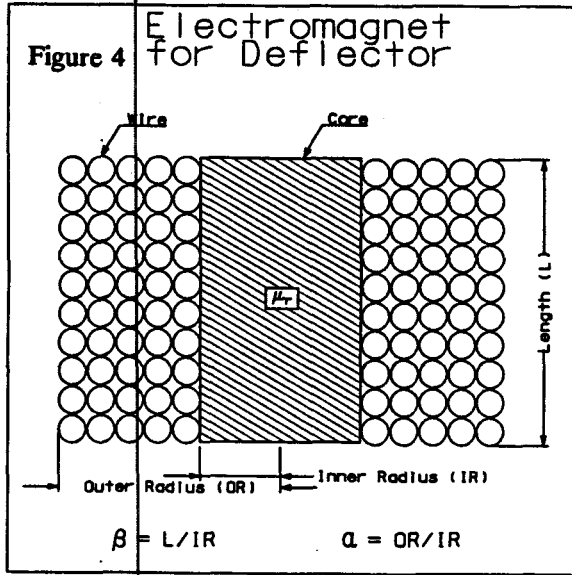


Figure 3





The parameters for this series of plots are:

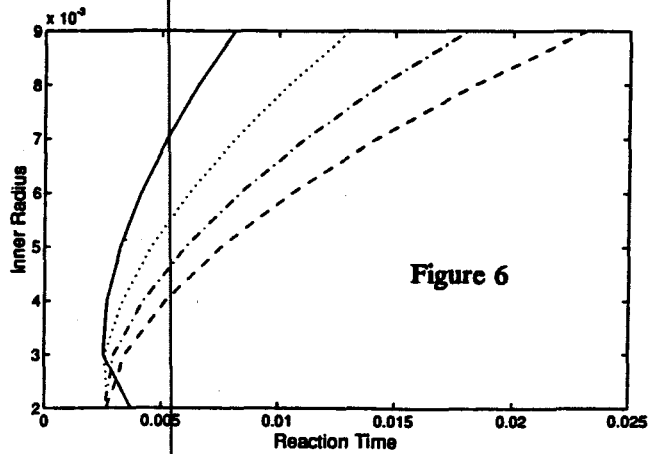
Electromagnet:  $\alpha = 2.5$   $\beta = 2.5$  Wire size = 22 AWG Current = 3.0 A

Deflector: Surface area = 72 mm<sup>2</sup> Mass = 2.0 g

Equivalent spring constant = 350 N/m

Inner Radius:

-- 3.0 mm - - 5.0 mm ..... 7.0 mm — 9.0 mm



The parameters for this series of plots is the same as above except:

Electromagnet:  $\alpha = 5$  Relative permeability = 5000

$\beta$ s:

-- 4.5 - - 3.5 ..... 2.5 — 1.5

**Table II** Summary of all test results showing the braided slit-film fabric versus the woven slit-film fabric

Test Type	Braided Fabric		Woven Fabric	
Cover Factor (%)	99.4		99.4	
Crimp Factor (%)	1.15		1.28	
Fabric Weight (oz/yd <sup>2</sup> )	2.90		1.95	
	warp	filling	warp	filling
Normalized Tensile Strength (lbs)	39.31	39.86	38.46	37.33
Normalized Fabric Elongation (%)	5.61	5.20	10.74	10.53
Normalized Shear Strength (lbs)	0.094	0.087	0.115	0.084
Tear Strength (g)	> 6,400		> 6,400	

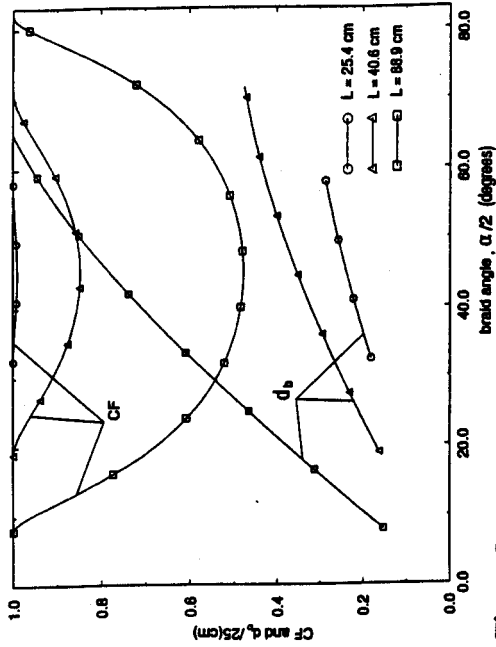


**Figure 8** Cover factor (CF) and braid diameter ( $d_b$ ) versus braid angle with different helical lengths. Number of carriers  $N_c = 192$ , yarn width  $w_y = 0.127 \text{ cm}$

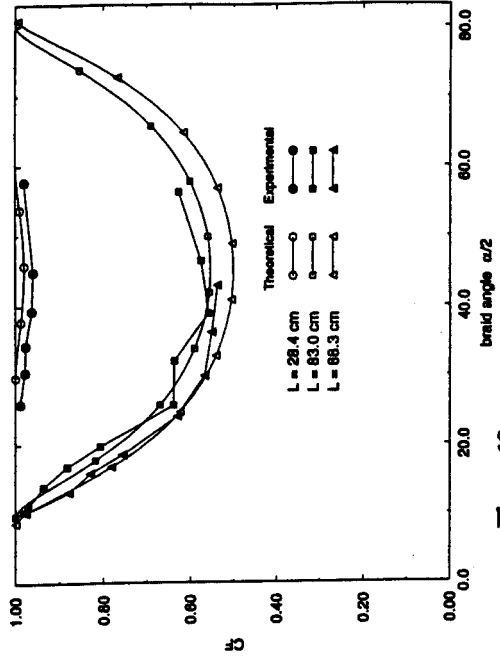


**Figure 10** Effect of braid angle on cover factor

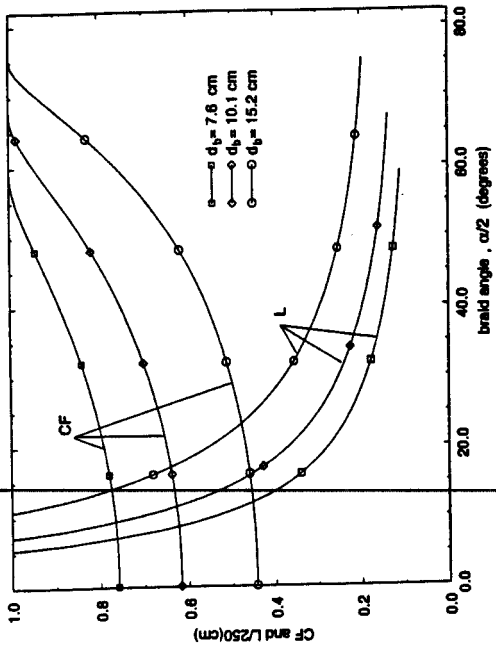


**Figure 7** Cover factor (CF) and helical length (L) versus braid angle ( $\alpha/2$ ) on 7.6 cm, 10.1 cm, and 15.2 cm mandrels. Number of carriers  $N_c = 192$ , yarn width  $w_y = 0.127 \text{ cm}$

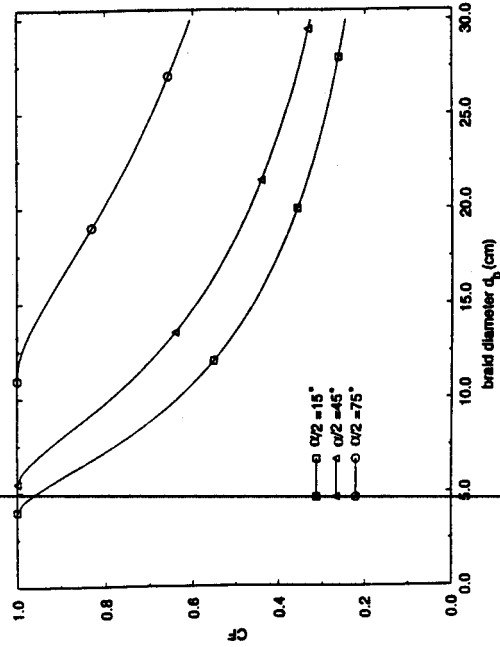


**Figure 9** Cover factor (CF) versus braid diameter ( $d_b$ ). Number of carriers  $N_c = 192$ , yarn width  $w_y = 0.127 \text{ cm}$